Application of the Local-Bulk Partitioning and Competitive Binding Models to Interpret Preferential Interactions of Glycine Betaine and Urea with Protein Surface†

Daniel J. Felitsky‡ and M. Thomas Record, Jr.*,‡,§

Department of Biochemistry and Department of Chemistry, University of Wisconsin-Madison, Madison, Wisconsin 53706

Received January 18, 2004; Revised Manuscript Received May 3, 2004

ABSTRACT: Two thermodynamic models have been developed to interpret the preferential accumulation or exclusion of solutes in the vicinity of biopolymer surface and the effects of these solutes on protein processes. The local-bulk partitioning model treats solute (and water) as partitioning between the region at/or near the protein surface (the local domain) and the bulk solution. The solvent exchange model analyzes a 1:1 competition between water and solute molecules for independent surface sites. Here we apply each of these models to interpret thermodynamic data for the interactions of urea and the osmoprotectant glycine betaine (*N*,*N*,*N*-trimethylglycine; GB) with the surface exposed in unfolding the marginally stable lacI HTH DNA binding domain. The partition coefficient K_P quantifying accumulation of urea at this protein surface ($K_P \cong 1.1$) is only weakly dependent on urea concentration up to 6 M urea. However, K_P quantifying exclusion of GB from the vicinity of this protein surface increases from 0.83 (extrapolated to 0 M GB) to 1.0 (indicating that local and bulk GB concentrations are equal) at 4 M GB (activity > 40 M). We interpret the significant concentration dependence of K_P for GB, predicted to be general for excluded, nonideal solutes such as GB, as a modest (8%) attenuation of the GB concentration dependence of solute nonideality in the local domain relative to that in the bulk solution. Above 4 M, K_P for the interaction of GB with the surface exposed in protein unfolding is predicted to exceed unity, which explains the maximum in thermal stability observed for RNase and lysozyme at 4 M GB (Santoro, M. M., Liu, Y. F., Khan, S. M. A., Hou, L. X., and Bolen, D. W. (1992) *Biochemistry 31*, 5278−5283). Both thermodynamic models provide good two-parameter fits to GB and urea data for lacI HTH unfolding over a wide concentration range. The solute partitioning model allows for a full spectrum of attenuation effects in the local domain, encompasses the cases treated by the competitive binding model, and provides a somewhat better two-parameter fit of effects of high GB concentration on lacI HTH stability. Parameters of this fit should be applicable to isothermal and thermal unfolding data for all proteins with similar compositions of surface exposed in unfolding.

Solute effects on protein, nucleic acid, and membrane processes are of universal importance throughout biochemistry and biology. Like ligands at mM concentrations or below, solutes at molar concentrations can exert either stabilizing or destabilizing effects on biopolymer processes (see reviews *1*, *2*, *3*). Unlike ligands at mM concentration, solutes at molar concentrations can exert large effects even if they exhibit little or no tendency to bind to or otherwise favorably interact with biopolymers, a situation called preferential hydration or exclusion (*1*−*3*). In the as-yet hypothetical case where a solute is completely excluded from the biopolymer surface affected in a process (complete preferential hydration), the effect of a solute would be a pure osmotic stress effect (*4*−*6*), resulting entirely from the reduction in activity of water with increasing solute concentration. Preferential exclusion of highly soluble, low molecular weight compounds called osmolytes from biopolymer surface has been proposed as the mechanism by which these molecules protect cells against the stress of high osmolality (*7*, *8*, *9*, and references therein). Glycine betaine (GB)[1] is a common osmolyte in both prokaryotic and eukaryotic cells; in E. coli, GB is the most effective osmolyte (osmoprotectant) characterized to date *(8*, *10)*.

For biopolymer processes, the consequences of preferential accumulation or exclusion of osmolytes and other small solutes (e.g., denaturants) at biopolymer surface are most directly and most fundamentally quantified by preferential interaction coefficients (*2*, *10*, *11*), which describe the effect of solute concentration on biopolymer activity coefficients.

Two quantitative thermodynamic models to interpret preferential accumulation or exclusion of solutes in the vicinity of biopolymer surface and to interpret or predict solute effects on biopolymer processes are the solute/H_2O competitive binding model of Schellman (*12*−*14*) and the local-bulk solute partitioning model of Record and coworkers (*11*, *15*−*17*). Both models provide a physical

† This research was supported by NIH grants GM47022 and GM23467. D. J. F. acknowledges support from a NSF predoctoral fellowship and a NIH Molecular Biosciences training grant.

* To whom correspondence should be addressed. 433 Babcock Dr., Madison, WI 53706. Tel.: 608-262-5332. Fax: 608-262-3453. E-mail: record@biochem.wisc.edu.

‡ Department of Biochemistry.

§ Department of Chemistry.

[1] Abbreviations: GB, glycine betaine; lacI DBD, lac repressor DNA-binding domain; HTH, helix-turn-helix domain; CD, circular dichroism.

10.1021/bi049862t CCC: $27.50
Published on Web 06/25/2004

interpretation of the thermodynamic consequences and structural basis of preferential accumulation or exclusion by incorporating hydration effects and invoking a division of water and solute between a region near the biopolymer surface and the bulk solution more distant from the biopolymer surface. The competitive binding model quantifies preferential interactions (accumulation or exclusion) using an equilibrium constant for the 1:1 exchange equilibrium between water and solute molecules for a denumerable set of sites on the biopolymer surface. With explicit treatment of a single class of independent, identical sites, the competitive binding model with two parameters (number of sites, competitive site binding/exchange constant) has successfully fit urea denaturation data of proteins (*18*) and in a modified form, urea denaturation of α-helical peptides (*19*). An extension of this model to include various excluded volume effects has very recently been proposed (*20*).

The partitioning model interprets preferential accumulation or exclusion of solutes in terms of a local-bulk partition coefficient for the solutes, characterizing partitioning of solute and water between a thermodynamically defined region near the biopolymer surface and the bulk solution. This solute partitioning model has been successfully applied to interpret urea and guanidinium chloride *m*-values (*15*), to analyze the effect of urea (*21*) on the thermodynamic and thermal stability of the small lacI HTH protein, and in its limiting form at low small solute concentration, to quantify interactions of osmolytes and denaturants with native BSA and other biopolymers (*11*, *22*). These models of preferential accumulation and exclusion of solutes have not previously been compared, and neither has been applied at very high concentrations of highly nonideal solutes such as GB.

Other approaches to interpret the thermodynamic consequences of solute-biopolymer preferential interactions are available, including statistical mechanical treatments based on Kirkwood−Buff theory (*23*−*25*). The different stabilizing effects of different excluded osmolytes (polyols) on the equilibrium constants of protein conformational changes have been analyzed by scaled particle theory (SPT) applied to a "hard" particle model for the solutes and solvent (*3*, *26*). Differences between observed and SPT-predicted effects have been attributed to "soft" interactions, such as hydrogen bonding, van der Waals, or dipole−dipole interactions. These soft interactions, which must be the dominant effect for all accumulated solutes such as urea, are also found to be very significant for the excluded solutes investigated.

In the current study, we examine the stabilization of the lacI helix-turn-helix domain (HTH) by the osmolyte glycine betaine (N, N, N-trimethylglycine; GB) over the range of GB concentration from 0.25 to 4.0 M. The marginal stability and reversible two-state unfolding of the small lacI HTH make it a valuable model system for the quantitative investigation of solute effects on protein processes (*21*); the thermodynamics of unfolding can be investigated over much wider ranges of temperature and solute concentration than is possible with larger, more stable proteins. GB is one of the most common osmolytes, found for example in bacteria, halophilic archaebacteria, marine invertebrates, plants, and kidneys of some mammalian species (*7*, *26*−*31*). In vitro, GB is found to be strongly excluded from native bovine serum albumin and lysozyme (*11*, *32*). Observed increases in thermal stability of several proteins with increasing GB concentration (*32*−*35*) indicate that GB is also preferentially excluded from the surface exposed upon unfolding. In the current study, preferential interaction coefficients obtained from lacI HTH unfolding experiments are analyzed using both the competitive binding model and the local-bulk partitioning model to obtain a quantitative measure of the local concentration deficit of this protein-stabilizing solute at the protein surface as a function of GB concentration and compared with previous analyses of the behavior of the destabilizing solute urea (*21*). Differences and similarities between these two models are discussed.

Background on Thermodynamics of Preferential Interactions. The model-independent thermodynamic expression for the dependence of the observed equilibrium constant for protein unfolding (or any other biopolymer process) on the activity (a_3) of a nonelectrolyte solute[2] such as urea or GB present in excess over the biopolymer components at constant temperature and pressure is

$$\left(\frac{\partial \ln K_{obs}}{\partial \ln a_3}\right)_{T,P,m_2} = \Delta\Gamma_{\mu 3} \tag{1}$$

where $\Delta\Gamma_{\mu_3}$ is the difference in preferential interaction coefficients Γ_{μ_3} characterizing the interaction of the solute with the unfolded and folded protein

$$\Gamma_{\mu_3} \equiv \left(\frac{\partial m_3}{\partial m_2}\right)_{T,P,\mu 3} = -\frac{(\partial\mu_2/\partial m_3)_{T,P,m_2}}{(\partial\mu_3/\partial m_3)_{T,P,m_2}} = -\left(\frac{\partial \ln \gamma_2}{\partial \ln a_3}\right)_{T,P,m_2} \tag{2}$$

In eq 2, chemical potentials μ_2 and μ_3 of biopolymer and small solute, respectively, are related to their molal concentrations m_2 and m_3 by $\mu_i = \mu_i^o + RT \ln a_i$, where $a_i = \gamma_i m_i$, and γ_i is the molal activity coefficient of species i. For macromolecular solutions, Γ_{μ_3} is approximately equal to the corresponding coefficient $\Gamma_{\mu_1\mu_3}$, describing the equilibrium distribution of the small solute (at constant chemical potential of water (μ_1) and small solute) across a dialysis membrane separating the ternary system from a two-component solution containing only water and the solute (*11*, *36*). If Γ_{μ_3} is nonzero, the distribution of the small solute in the vicinity of the biopolymer is nonuniform, and a gradient (positive or negative) in its concentration exists between the biopolymer surface and the bulk solution.

(*a*) *Interpretation of* Γ_{μ_3} *and* $\Delta\Gamma_{\mu_3}$ *Using the Local-Bulk Solute Partitioning Model.* The local-bulk partitioning model is based on a two-domain interpretation of the solute concentration gradient, with local and bulk molal concentrations m_3^{local} and m_3^{bulk}. m_3^{bulk} is defined to be equal to that in the two-component solution that would be in dialysis equilibrium with the ternary system if a semipermeable membrane were introduced. The molality of solute in the vicinity of the biopolymer, m_3^{local}, differs from m_3^{bulk} because of differences in the strength of interaction of the biopolymer with the perturbing solute as compared to the strength of interaction of both species with water. Quantitative treatment of the two-domain description of preferential interactions provides the following interpretation of the preferential

[2] Numerical subscripts designate water (1), biopolymer (2), and small solute (3), respectively.

interaction coefficient

$$\Gamma_{\mu_1\mu_3} = B_3 - m_3^{\text{bulk}}\frac{B_1}{m_1^\bullet} = (m_3^{\text{local}} - m_3^{\text{bulk}})\frac{B_1}{m_1^\bullet} \cong \Gamma_{\mu_3} \quad (3)$$

where B_1 and B_3 are the numbers of water molecules and small solute molecules in the local domain per molecule of biopolymer ($B_3/B_1 = m_3^{\text{local}}/m_1^\bullet$) and $m_1^\bullet = 55.5$ mol H_2O/kg. Equations 2 and 3 indicate that, for excluded solutes where $m_3^{\text{local}} < m_3^{\text{bulk}}$ and therefore $\Gamma_{\mu_3} < 0$, the biopolymer activity coefficient increases as the concentration of the small solute increases, and therefore that solute-biopolymer interactions are unfavorable relative to the ideal dilute solution state where both solute and biopolymer interact only with water.

For uncharged solutes, and even for salts at sufficiently high concentration (*15*), m_3^{local} is related to the bulk concentration m_3^{bulk} by a solute partition coefficient K_P

$$K_P \equiv \frac{m_3^{\text{local}}}{m_3^{\text{bulk}}} = \frac{(X_3/X_1)^{\text{local}}}{(X_3/X_1)^{\text{bulk}}} \quad (4)$$

where X_3^{local}, X_1^{local}, X_3^{bulk}, X_1^{bulk} are local and bulk mole fractions of small solute (subscripted 3) and water (subscripted 1). Partitioning of solute into the local domain displaces water and reduces B_1

$$B_1 = B_1^o - S_{1,3}B_3 \quad (5)$$

where B_1^o is the number of waters hydrating the biopolymer (i.e., in the local domain) in the absence of GB, and $S_{1,3}$ is the cumulative stoichiometry of exchange. From eqs 3−5

$$\frac{\Gamma_{\mu_3}}{m_3^{\text{bulk}}} = \frac{(K_P - 1)B_1^o}{m_1^\bullet(1 + K_P S_{1,3} m_3^{\text{bulk}}/m_1^\bullet)} \quad (6)$$

At low to moderate m_3, where $K_P S_{1,3} m_3^{\text{bulk}} \ll m_1^\bullet$, eq 6 predicts that Γ_{μ_3} is proportional to m_3^{bulk} if K_P is concentration independent. Evidence for this is provided by the concentration independent values of $\Gamma_{\mu_3}/m_3^{\text{bulk}}$, determined experimentally for a variety of protein-solute interactions in the range of 0−1 molal solute (*11*, *22*).

What is B_1^o and how does it vary with the water accessible surface area of the biopolymer? The local-bulk domain model interpretation of Γ_{μ_3} (eq 6) was used in a rigorous thermodynamic analysis (*15*) of the significant observation by Myers, Pace, and Scholtz (*37*) that urea and guanidinium chloride *m*-values are directly proportional to the protein surface area (ASA) exposed to solvent in unfolding. From this analysis, we concluded that B_1^o is proportional to surface area for a homologous series of biopolymer surfaces

$$B_1^o = b_1^o \text{ ASA} \quad (7)$$

where the proportionality constant b_1^o is the average number of water molecules per unit of protein surface. Different (nonhomologous) types of biopolymer surface may exhibit quite different hydrations b_1^o. Analyses of preferential interactions between native proteins and the most strongly excluded solutes yield minimum estimates of b_1^o of less than a monolayer of hydration. Thus, as a working hypothesis, the thermodynamically relevant hydration (B_1^o) was proposed to be on average a monolayer of water at the protein surface ($b_1^o = 0.11$ $H_2O/Å^2$ (*15*)) to estimate solute partition coefficients K_P. If this estimate of b_1^o were incorrect, values of ($K_P - 1$) would be changed proportionately (see eq 6−7).

For protein unfolding in a large excess of the small solute (where $m_3^{\text{bulk}} \cong m_3 \gg m_2$), the dependence of the observed equilibrium constant on the molality of solute (GB, urea, etc.) is interpreted as

$$\text{(partitioning model)}\ \frac{\partial \ln K_{\text{obs}}}{\partial m_3} = -\frac{1}{RT}\frac{\partial \Delta G^\circ_{\text{obs}}}{\partial m_3} = \frac{(K_P - 1)(1 + \epsilon_3^m)}{m_1^\bullet(1 + K_P S_{1,3} m_3/m_1^\bullet)} b_1^o \Delta\text{ASA} \quad (8)$$

where ΔASA is the protein surface area exposed upon unfolding ($\Delta\text{ASA} = \text{ASA}^U - \text{ASA}^F$) and the quantity ($1 + \epsilon_3^m$), obtainable from two-component osmolality or molal scale activity coefficient (γ_3) data on the small solute, arises from the conversion from an activity derivative to a molality derivative ($\epsilon_3^m = \partial \ln \gamma_3/\partial \ln m_3$).

(*b*) *Interpretation of* Γ_{μ_3} *and* $\Delta\Gamma_{\mu_3}$ *Using the Solute/H_2O Competitive Binding Model.* The solute/H_2O competitive binding model has been derived (*14*) from a binding polynomial analysis utilizing a symmetric treatment of water and solute. For each site at the biopolymer surface, equilibria are formulated for binding water and solute

$$H_2O + P_0 \leftrightarrow P_1 \quad K_1 \equiv \frac{[P_1]}{[P_0]a_1} \quad (9A)$$

$$\text{solute} + P_0 \leftrightarrow P_3 \quad K_3 \equiv \frac{[P_3]}{[P_0]a_3} \quad (9B)$$

where P_0 refers to an unoccupied site, and P_1 and P_3 indicate occupation of a site on the biopolymer surface by water and solute, respectively (*12*). The equilibrium constants K_1 and K_3 are defined in terms of mole fraction concentrations and activities of solute and water. The binding polynomial for the site (or equivalently the semi-grand canonical partition function (*14*))

$$\sum \equiv 1 + K_1 a_1 + K_3 a_3 \cong K_1 a_1 + K_3 a_3 \quad (10)$$

contains contributions from both hydration and solute binding; in solution, the site is assumed always to be occupied by water or solute ($K_1 a_1$, $K_3 a_3 \gg 1$) (*14*). Incorporating hydration into the ideal dilute solution standard state chemical potential of the biopolymer gives the following expression for the biopolymer mole fraction activity coefficient:

$$f_2 = \frac{K_1}{\Sigma} = \frac{1}{a_1 + K_{\text{site}} a_3} \quad (11)$$

where K_{site}, the equilibrium constant for exchanging H_2O with solute at the site, is directly related to the equilibrium constants for site occupancy

$$K_{\text{site}} \equiv \frac{[P_3]a_1}{[P_1]a_3} = \frac{K_3}{K_1} \quad (12)$$

In a recent application of this model, the activities a_1 and a_3 have been approximated by volume fractions (*38*). To interpret the dependence of the observed equilibrium constant for a biopolymer process on the molality of solute without overparametrizing the model, it is necessary to assume a single set of N independent sites with identical exchange constants (K_{site})

$$\text{(binding model)}\frac{\partial \ln K_{obs}}{\partial m_3} = \frac{1}{RT}\frac{\partial \Delta G^{\circ}_{obs}}{\partial m_3} = \frac{\left(K_{site}\frac{f_3}{f_1} - 1\right)}{m_1^{\bullet}\left(1 + K_{site}\frac{f_3}{f_1}\frac{m_3}{m_1^{\bullet}}\right)}(1 + \epsilon_3^m)N \quad (13)$$

where the definition of $(1+\epsilon_3^m)$ is identical to that following eq 8 and the relatively small difference between mole fraction and molal activity coefficients for the solute is neglected ($f_3 = \gamma_3/X_1$). Equation 13, derived for 1:1 exchange and for the situation where solute and solvent nonideality is introduced in the free (bulk) state but not the bound (local) state, corresponds as expected to eq 8 for the situation where $S_{1,3}$=1 (i.e., 1:1 exchange), $B_1^o = b_1^o\Delta$ASA=N, and $K_P = K_{site}(f_3/f_1)$. Because K_{site} is presumed to be concentration invariant, eq 13 is analytically integrable (in contrast to eq 8), giving

$$\text{(binding model)}\ \ln K_{obs} = -\Delta G^{\circ}_{obs}/RT = \ln K_{obs}(m_3 = 0) + N\ln(a_1 + K_{site}a_3) \quad (14)$$

MATERIALS AND METHODS

Circular dichroism spectroscopy studies and two-state equilibrium analysis of the urea and GB dependence of lacI HTH unfolding are described in detail elsewhere (*21*; Felitsky et al., submitted). Urea activity coefficients and molalities were calculated as described previously (*21*). GB molalities were calculated from molar concentrations at 23 °C using a value of $\bar{V}_3 = 0.0982$ (*11*). GB activity coefficients on the molal scale (γ_3) were calculated from isopiestic distillation data at 25 °C (0.1−4.94 molal) (*39*) using the Gibbs−Duhem relation (*40*). For GB concentrations up to 4.94 m, values of ln γ_3 are best fitted by a cubic polynomial in m_3

$$\ln \gamma_3 = \Sigma\beta_i m_3^i \quad (15)$$

with coefficients $\beta_1 = 0.347546$, $\beta_2 = -1.01255 \times 10^{-2}$, and $\beta_3 = 7.54385 \times 10^{-4}$. Molal activity coefficients of GB solutions at higher concentrations (in the range 5−7 molal) were estimated by extrapolation of this fitting equation. (For example, γ_3 equals 3.37 at 3.8 m and 4.76 at 4.94 m and is estimated to be 6.57 at 6 m, and 7.96 at 6.61 m GB.) Mole fraction activity coefficients of GB (f_3) are obtained from molal activity coefficients (γ_3) at 25 °C using the equation $f_3 = X_1^{-1}\gamma_3$, where X_1 is the mole fraction of water.

Water activities at different GB concentrations were calculated directly from the practical osmotic coefficients φ reported by Smith and Smith (*39*) by the relationship $\varphi m_3 \equiv$ osmolality $= -m_1^{\bullet}\ln a_1$ and used to obtain mole fraction activity coefficients of water at 25 °C ($f_1 = a_1/X_1$). To our knowledge, no information exists regarding the temperature dependence of the activity coefficient of GB. Osmotic coefficients determined from osmometric (VPO) measurements on binary (GB, water) solutions at 25 °C and 37 °C (Mike Capp, Pers. comm.) exhibit no detectable temperature dependence. In our analysis, we therefore assume that the activity coefficient of GB is independent of temperature. With this assumption, molar and molal activities are numerically identical, and the molar scale activity coefficient γ_3^c can be obtained from $\gamma_3^c = a_3/C_3$, where a_3 and C_3 are the molar scale activity and molarity of the solute, respectively.

Water Accessible Surface Area (*ASA*) *Calculations.* The area of the folded state of lacI HTH was calculated as the average of the first 51 residues of all 11 NMR models in the file 1CJG in the Protein Data Bank (www.rcsb.org). The unfolded state of these 51 residues was modeled as an extended β-chain using Insight II (Biosym Technologies). (An alternative model consisting of an elongated polyproline II helix was examined; calculations for this structure (DJF, not shown) yield an essentially identical estimate of ASA for the unfolded protein.) Water-accessible surface areas of these protein structures were calculated using SurfRace (*41*), with a probe radius of 1.4 Å and accepted values of the van der Waals radii (set I; *42*). These calculations yield ΔASA = 3465 Å^2, which is ∼13% smaller than that of PDB file 1LQC, which was used in our previous ASA calculations. We have since recognized that many charged groups on side chains in the structure used previously are modeled as being buried in the native state, leading to an overestimate of ΔASA of unfolding.

One-Parameter Model Fits. The one-parameter fit of the local-bulk solute partitioning model using eq 8 was applied to urea denaturation with $S_{1,3} = 2.7$ and $b_1^o = 0.11$ H$_2$O/Å^2, as described previously (*21*) with ΔASA = 3465 Å^2 (see above). While an analogous procedure was used in fitting this model to the GB concentration dependence of ln K_{obs}, only data below 1.25 M GB were fitted, because inclusion of data at higher GB concentrations resulted in deviations of the one-parameter partitioning fit from the observed GB-concentration dependence in the dilute solution limit. For GB, the same average protein hydration per unit surface ($b_1^o = 0.11$) was assumed, eq 15 was used to quantify the GB molal activity coefficient, and the water-solute exchange stoichiometry $S_{1,3}$ was fixed at 2.2 (calculated from the ratio of the cross sectional area of GB and water modeled as spheres (*43*) by the method of Edward (*44*)). For the one-parameter (K_{site}) fit of the competitive binding model using eq 14, individual sites were assumed to cover 9.1 Å^2 (i.e. 0.11^{-1}) of surface exposed in unfolding, fixing N at 3465/9.1 = 381 sites. For the same reason described above for the local-bulk GB partitioning fit, only data below 1.0 M GB and 1.6 M urea were fitted in applying the one-parameter competitive binding model.

Two-Parameter Model Fits. To apply the two-parameter (K_P^o and α) local-bulk solute partitioning model to the unfolding data, the fitting procedure involved numerically solving eq 21 for a given set of parameter values, incorporating the resulting K_P into eq 8, and numerically integrating eq 8. The process was repeated iteratively using a nonlinear regression program until a best fit set of parameters was

Table 1: ln K_{obs} and ΔG°_{obs} for Isothermal Unfolding of lacI HTH at 59 °C

C_3[a]	m_3	a_3[b] (molar)	a_1 (mole fraction)	a_3 (mole fraction)	ln K_{obs}	ΔG°_{obs} kcal mol^{-1}
0.00	0.00	0.00	1.000	0.000	1.94 ± 0.85	−1.28 ± 0.56
0.25	0.26	0.28	0.996	0.005	1.86 ± 0.13	−1.23 ± 0.08
0.50	0.53	0.63	0.990	0.011	1.56 ± 0.16	−1.03 ± 0.11
0.75	0.81	1.07	0.983	0.019	1.05 ± 0.26	−0.69 ± 0.17
1.00	1.11	1.62	0.976	0.029	0.75 ± 0.47	−0.50 ± 0.31
1.25	1.43	2.31	0.968	0.042	0.68 ± 0.28	−0.45 ± 0.19
1.50	1.76	3.17	0.960	0.057	0.29 ± 0.10	−0.19 ± 0.07
1.75	2.12	4.26	0.950	0.077	−0.05 ± 0.12	0.03 ± 0.08
2.00	2.50	5.65	0.939	0.102	−0.38 ± 0.22	0.25 ± 0.14
2.25	2.90	7.42	0.927	0.134	−0.70 ± 0.09	0.46 ± 0.06
2.50	3.32	9.71	0.913	0.175	−1.02 ± 0.03	0.67 ± 0.02
2.75	3.78	12.68	0.897	0.228	−1.18 ± 0.10	0.78 ± 0.07
3.00	4.27	16.59	0.880	0.299	−1.47 ± 0.94	0.97 ± 0.62
3.25	4.79	21.81	0.860	0.393	−1.57 ± 0.41	1.04 ± 0.27
3.50	5.35	28.89[c]	0.838[c]	0.521[c]	−1.76 ± 0.19	1.16 ± 0.13
3.75	5.96	38.70[c]	0.812[c]	0.697[c]	−1.98 ± 0.32	1.30 ± 0.21
4.00	6.61	52.61[c]	0.782[c]	0.937[c]	−2.50 ± 0.41	1.65 ± 0.27

[a] C_3 is the molar GB concentration. [b] Differences between molar and molal GB activities are negligible. $a_3 = \gamma_3^m m_3$, where γ_3^m was evaluated from analysis of isopiestic distillation data as described in Methods. [c] Extrapolated (see Methods).

obtained. Values of b_1^o, $S_{1,3}$, and ΔASA were identical to those used in the one-parameter fits above. The two-parameter competitive binding model was applied using eq 14 and floating both N and K_{site}. Nonlinear regression was performed using a modified version of the Marquardt algorithm of Bevington and Robinson (*45*).

RESULTS

Analysis of Isothermal Folding of lacI HTH with Increasing Glycine Betaine or Urea Concentration: Implications of Solute Concentration Independent m-Values. The quantities ln K_{obs} and ΔG°_{obs} for lacI HTH unfolding as a function of GB concentration have been determined over the temperature range from ∼37 to ∼80 °C (Felitsky et al., submitted). Values of K_{obs} (and the *m*-value, defined as $-d\Delta G^{\circ}_{obs}/dC_3$, where C_3 is the molarity of GB) are experimentally determined over the widest range of GB concentrations and therefore most valuable for testing the applicability of theoretical models in the middle of this temperature range. The dependences of ΔG°_{obs} and ln K_{obs} for lacI HTH unfolding at 59.0 °C on GB concentration and activity are tabulated in Table 1 and plotted as a function of GB molarity in Figure 1A. In the absence of GB, lacI HTH is almost completely unfolded at this temperature. The addition of 3.75 M GB at 59.0 °C reduces K_{obs} for unfolding to 1/50 of its value in the absence of GB, stabilizing the folded protein by 2.6 kcal mol^{-1}. At the same temperature and buffer conditions, for comparison, K_{obs} in 3.75 M urea is predicted to be 20-fold larger than in the absence of urea, corresponding to a destabilization of the folded protein of 2.0 kcal mol^{-1} (*21*). Figure 1A shows that the dependence of ΔG°_{obs} on GB molarity is approximately linear up to at least 3 M GB, with a constant *m*-value of −790 ± 30 cal mol^{-1} M^{-1}; the *m*-value appears to decrease slightly in magnitude above 3 M GB. For comparison, the dependences of ΔG°_{obs} and ln K_{obs} for lacI HTH unfolding at 37 °C on urea concentration from 0.0 to 6.0 M are plotted in Figure 1B using previously published data (*21*); ΔG°_{obs} is well described as a linear function of urea molarity over the entire range of experimentally accessible urea concentrations. (The urea dependence of ΔG°_{obs} is only measurable at low urea concentrations at 59 °C, but is predicted to be linear over the aforementioned 6 M range with a slightly smaller *m*-value (*21*).)

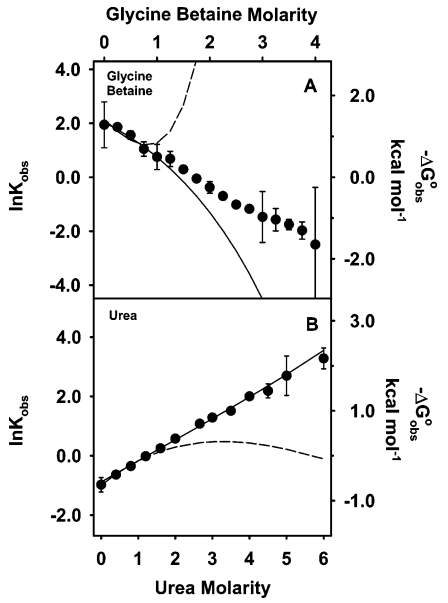

FIGURE 1: Dependence of ln K_{obs} for lacI HTH unfolding on GB (panel A; 59 °C) and urea (panel B; 37 °C) molarity. One-parameter fits are shown for the local-bulk solute partitioning model with a constant K_P (—) and the competitive binding model with a constant K_{site} (− − −). The fit to the urea data was obtained as in reference (*21*).

For urea, the one-parameter local-bulk solute partitioning model with a concentration-independent K_P (eq 4) predicts that a plot of ΔG°_{obs} vs urea molarity will be linear and that the *m*-value will be constant within uncertainty up to at least 6 M and yields $K_P = m_3^{local}/m_3^{bulk} = 1.11 \pm 0.01$ (Figure 1B) (*15*, *21*). The analogous one-parameter fit to the competitive binding model with the number of sites $N = b_1^o\Delta ASA$ fixed at the value expected for hydration of the entire ΔASA for lacI HTH unfolding, is acceptable up to ∼1.5 M urea with a best-fit $K_{site} = 1.15 \pm 0.04$ (Figure 1B), but deviates significantly above 1.5 M. For this same choice of hydration, neither model gives a good one-parameter fit for the GB-

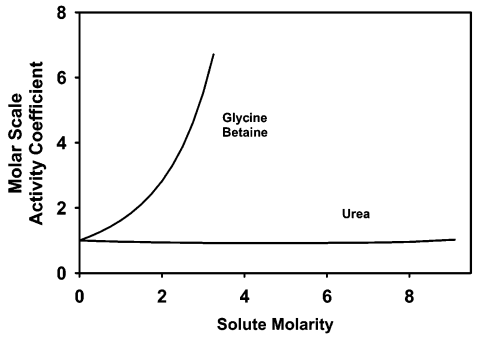

FIGURE 2: Molar scale activity coefficients for aqueous GB and urea binary solutions as a function of solute molarity.

induced folding of lacI HTH; the two fits deviate from the experimental data in opposite directions. The competitive binding model with a best-fit $K_{site} = 0.73 \pm 0.12$ shows a positive deviation from the experimental data at relatively modest (<0.75 M) GB concentrations and predicts a changeover from stabilization to GB-induced destabilization of lacI HTH at ~1 M GB, entirely due to GB-concentration-dependent nonideality. (Such a changeover does apparently occur, but only above 4 M as discussed below.) No other plausible choice for the extent of hydration (i.e. N) affects these conclusions; only if N is chosen as a small subset of hydration water do the fits to the competitive binding model improve (see below). The local-bulk solute partitioning model with a constant partition coefficient ($K_P = 0.85 \pm 0.07$) predicts significant downward curvature above ~1 M GB in the plot of ln K_{obs} versus molar GB concentration (Figure 1A), and a greater stabilization of the folded state of lacI HTH by GB than is observed experimentally. Intriguingly, deviations of the one-parameter fits from the experimental data are much more pronounced with GB than with urea for both models.

The extended linearity of the plot of ln K_{obs} or ΔG°_{obs} versus molar GB concentration and the constant GB *m*-value in Figure 1A, while incompatible with the one parameter fits to either the binding or partitioning model, is empirically consistent with the behavior observed for most proteins in urea and GuHCl (Figure 1B) (*21*, *46*, *47*, *48*). The extended linearity observed for urea can be rationalized because the activity coefficient of urea on the molar scale is relatively independent of urea concentration (see Figure 2). Therefore, urea solutions do not deviate greatly from ideal dilute solution behavior on this concentration scale over the concentration range of interest, and the molarity axis in Figure 1B is similar to an activity scale. By contrast, for GB, γ_3^c is a highly nonlinear function of molarity, increasing strongly as its molar concentration is increased (Figure 2). Indeed, the thermodynamic nonideality of GB at 25 °C increases very strongly on all concentration scales with increasing GB concentration in the range of the isopiestic distillation data (0.1−3.25 M; *39*). At a concentration of 3.25 M, the molar scale activity (i.e., effective concentration) of GB is 22 M and at 3.75 M is estimated to be 38.7 M, approximately equal to the molarity of water in this solution as calculated from the partial molar volumes of water and GB. Therefore, the extended linearity of a plot of ΔG°_{obs} versus molar GB concentration (Figure 1) is initially difficult to understand from basic thermodynamic principles; an extension of the solute partitioning model to include differences in solute nonideality in local and bulk domains suffices to explain this behavior as described in the Discussion.

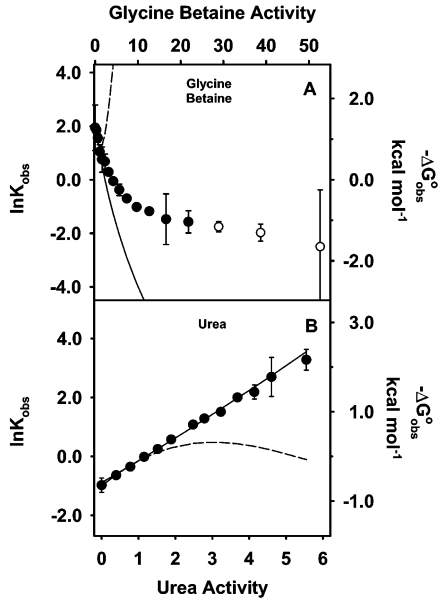

FIGURE 3: Dependence of ln K_{obs} for lacI HTH unfolding from Figure 1 replotted against the thermodynamic activity of GB (panel A; 59 °C) and urea (panel B; 37 °C). Fitted curves are as in Figure 1.

Figure 3 replots the data of Figure 1 for GB and urea on a molar activity scale. The plot of ln K_{obs} or ΔG°_{obs} for unfolding versus activity of urea (Figure 3B) is linear with virtually the same slope as Figure 1B. However, ΔG°_{obs} for folding is a highly nonlinear function of GB activity, exhibiting an approach to a plateau (or local maximum in thermodynamic stability) at GB activities above 20 M. This behavior could be interpreted simply as saturable binding of GB to the folded form of lacI HTH (without considering exchange), and indeed the data of Figure 3A are well-fit with a single site for GB on the folded HTH (site binding constant of 2.5 M^{-1}). GB also modestly increases the thermal stability of a variety of other proteins (*33*, *34*, *49*) unrelated to lacI HTH; these effects could also be interpreted as site binding of GB to a single site or small number of sites on the native conformations of these proteins. However, these site binding models are implausible because GB is found to be quite strongly excluded from native protein (BSA, lysozyme) surface (K_P~0.5 (*11*, *32*)) and because it is unlikely that GB has a single binding site of significant affinity on all of these unrelated proteins. (Various of these proteins, including bovine pancreatic RNase A and chicken egg white lysozyme, presumably do not encounter GB at molar concentrations in vivo and thus have no obvious use for such a site.) Therefore, consistent with previous qualitative interpretations (*32*−*34*) of osmolyte effects on protein unfolding, we quantify the thermodynamic stabilization of the folded state of lacI HTH in terms of preferential exclusion of GB from the surface exposed in the unfolding process.

DISCUSSION

Figures 1 and 3 indicate that neither model (competitive 1:1 binding, partitioning) provides an adequate one-parameter (binding constant, partition coefficient) fit to the lacI HTH stability data as a function of GB concentration or activity,

Table 2: Partitioning Model: Divisions of Molecular Interactions in Bulk and Local Domains

	interactions that contribute to the standard state chemical potential	interactions that contribute to local and bulk activity coefficients			
	(identical for both local and bulk domains)	in bulk solution		in the local domain (vicinity of protein)	
		dilute in solute	more concentrated	dilute in solute	more concentrated
solute	only solute−solvent (ideal dilute) interactions	none	solute−solute interactions	solute−protein interactions	solute−protein interactions solute−solute interactions
solvent (H_2O)	only solvent−solvent (ideal) interactions	none	solvent−solute interactions	solvent−protein interactions	solvent−protein interactions solvent−solute interactions

when the number of bound water molecules is set equal to a monolayer coverage of the surface exposed in unfolding. Both models are more successful in treating the urea dependence of lacI HTH stability for the same choice of hydration number with single-parameter fits, although the competitive binding model still deviates strongly from the experimental data at moderate to high urea concentrations.

It is reasonable to conclude that the greater deficiencies of both models in fitting GB effects relative to their abilities to fit the urea data result from inadequate treatments of thermodynamic nonideality, which is pronounced for GB but less consequential for urea. Since the two models fail in opposite ways for GB, it is also reasonable to conclude that one overcorrects and the other undercorrects for solute-concentration dependent nonideality. The partitioning model, which neglects concentration-dependent nonideality in the definition of the partition coefficient, and therefore implicitly assumes that this nonideality has the same dependence on bulk solute concentration in local and bulk domains (see below), provides a better fit to both urea and GB data than does the competitive binding model, which explicitly includes concentration-dependent nonideality for free solute and water but of necessity neglects it for bound solute and water. Indeed, the concentration-dependent nonideality of unbound solute and water is also neglected in the most recent application of the binding model (*20*).

Motivated by these failings of both models at high concentrations of GB, we formulate a general thermodynamic description of partitioning which includes nonideality effects in both domains and which relates the concentration dependences of nonideality in the two domains using the previously proposed concept of attenuation of solute−solute nonideality (*13*) as a result of interactions with the biopolymer in the local domain.

Extension of the Solute Partitioning Model to Include Solute-Concentration Dependent Nonideality in the Local Domain. The local-bulk partition coefficient K_P of eq 4 was originally introduced (*11*) to relate m_3^{local} to m_3^{bulk} in eq 3. Here, by treating local-bulk partitioning of solute as phase partitioning between a local domain and the bulk solution (i.e., the region of solution sufficiently distant from the protein surface that solute and water are thermodynamically unperturbed by the protein), we clarify the physical connection between K_P and both local and bulk nonideality. For the phase partitioning process, the condition for thermodynamic equilibrium is the equality of the chemical potential of each species (solute or solvent) in the two domains. We define the standard state chemical potential of solute identically for both local and bulk domains as the chemical potential for the hypothetical (ideal dilute solution) standard state in which solute at unit mole fraction (i.e., pure solute) experiences the same intermolecular forces it experiences when in extremely dilute solution in the absence of the protein. This choice of standard state has the effect of incorporating interactions between the protein and solute into the local domain activity coefficient (Table 2). The condition for thermodynamic equilibrium then reduces to an equality of local and bulk activities

$$a_1^{local} = (f_1X_1)^{local} = (f_1X_1)^{bulk} = a_1^{bulk}$$
$$a_3^{local} = (f_3X_3)^{local} = (f_3X_3)^{bulk} = a_3^{bulk} \quad (16)$$

where f_i is the mole fraction scale activity coefficient of component i. Both bulk activity coefficients approach unity as X_1^{bulk} approaches unity, using the ideal dilute solution reference state for the solute. Local activity coefficients will differ from unity even as X_1^{local} approaches unity as a consequence of interactions of solute and water with the protein surface. Table 2 catalogues the species and types of molecular interactions present in the local and bulk regions. At equilibrium, a thermodynamic partition coefficient defined in terms of local and bulk activities

$$K_{EQ} \equiv \frac{(a_3/a_1)^{local}}{(a_3/a_1)^{bulk}} = \frac{(f_3/f_1)^{local}}{(f_3/f_1)^{bulk}} \frac{(X_3/X_1)^{local}}{(X_3/X_1)^{bulk}} = 1 \quad (17)$$

has a constant value of unity, independent of solute concentration. Equation 17 demonstrates that any difference in the quotient of solute and water activity coefficients between the local and bulk domains necessarily alters the local concentrations of solute and water near the protein relative to their bulk concentrations and hence determines K_P, defined as in eq 4

$$K_P \equiv \frac{(X_3/X_1)^{local}}{(X_3/X_1)^{bulk}} = \frac{(f_3/f_1)^{bulk}}{(f_3/f_1)^{local}} \quad (18)$$

Moreover, any difference in the dependences of the local and bulk activity coefficient ratios on bulk solute concentration will cause K_P to be solute concentration dependent.

At low solute concentration, where $f_3^{bulk} = f_1^{bulk} = 1$, K_P takes on the limiting value K_P^o defined as

$$K_P^o \equiv f_1^{o,local}/f_3^{o,local} \quad (19)$$

where $f_1^{o,local}$ and $f_3^{o,local}$ are activity coefficients in the local

Table 3: Behaviors Associated with Attenuation of Solute Concentration Dependent Nonideality in the Local Domain Relative to That in the Bulk Domain in the Partitioning Model

$\alpha \equiv \alpha_1 = \alpha_3$	thermodynamic behavior	physical situation	potentially invariant (solute concentration independent) partition coefficient
$\alpha = 0$	local nonideality is independent of solute concentration	independent site binding; solute molecules isolated in protein cavities; approximate treatment for systems with interactions in the local domain	K_P' (invariant if $\alpha = 0$) (eq 23)
$0 < \alpha < 1$	local nonideality depends less strongly on solute concentration than does bulk nonideality	anticipated behavior for both weakly accumulated and weakly excluded solutes; protein partially occludes solute surface or otherwise competes for solute interactions	K_P (invariant for an accumulated solute if $K_P \cong 1/\alpha_3 > 1$)
$\alpha = 1$	local and bulk nonidealities have identical dependences on solute concentration	relevance to real systems is limited	K_P (invariant for an inert solute if $K_P \cong 1/\alpha_3 \cong 1$)
$\alpha > 1$	local nonideality depends more strongly on solute concentration than does bulk nonideality	relevance to real systems is unlikely; unfavorable (favorable) solute−solute interactions are increased near the biopolymer surface	K_P (invariant for an excluded solute if $K_P \cong 1/\alpha_3 < 1$)
$\alpha < 0$	local nonideality has opposite dependence on solute concentration from that in bulk solution nonideality	relevance to real systems is unlikely; solute−solute interactions are unfavorable (favorable) in bulk solution but favorable (unfavorable) near the biopolymer	none

domain in the limit where the nonideality of solute in the local domain arises from its interactions with protein surface but not from interactions with other solutes, and likewise where the interactions of water in the local domain are almost entirely with water and protein, and not with solute. (This is the analogue of the ideal dilute solution reference state used in the bulk domain; Table 2.) We propose that for weakly interacting solutes, any deviation of the ratio $(f_3/f_1)^{local}$ from its limiting value $(K_P^o)^{-1}$ with increasing bulk solute concentration results from solute−solute interactions similar to those that cause $(f_3/f_1)^{bulk}$ to deviate from its ideal dilute solution value of unity. To account for these concentration dependent differences, we define the quantities α_1 and α_3

$$\left.\frac{d\ln f_1^{local}}{dm_3^{local}}\right|_{m_3^{local}=m_3^*} \equiv \alpha_1 \left.\frac{d\ln f_1^{bulk}}{dm_3^{bulk}}\right|_{m_3^{bulk}=m_3^*}$$

$$\left.\frac{d\ln f_3^{local}}{dm_3^{local}}\right|_{m_3^{local}=m_3^*} \equiv \alpha_3 \left.\frac{d\ln f_3^{bulk}}{dm_3^{bulk}}\right|_{m_3^{bulk}=m_3^*} \quad (20)$$

where the proportionality between the two derivatives requires that they be evaluated at the same solute concentration m_3^*, even though the constraints $m_3^{local} = m_3^*$ and $m_3^{bulk} = m_3^*$ are not satisfied simultaneously in solution. Application of the Gibbs−Duhem equation to both bulk and local macroscopic domains gives the result $\alpha_3 = \alpha_1 \equiv \alpha$. Because solute and H_2O in the local domain interact with the protein surface, the solute concentration dependence of nonideality in the local domain is expected to be reduced (attenuated) relative to that of the bulk solution (i.e., α should be less than unity) by an amount that is determined by both the strength of the solute−protein interaction and the extent to which the protein obstructs or disrupts solute−solvent interactions in the local domain (e.g., by sterically occluding solute/H_2O functional groups or restricting orientations of molecules).

Only in the unlikely case where $\alpha = 1$ will the dependence of the excess free energy in bulk solution (f_i^{bulk}) on the bulk solute concentration m_3^{bulk} be identical to the dependence of the local excess free energy (f_i^{local}) on the local solute concentration m_3^{local}. In this case ($\alpha = 1$), the presence of the biopolymer would not perturb the concentration dependence of solute−solute interactions, although the local solute concentration would generally differ from the bulk solute concentration (i.e., $K_P \neq 1$).

If the solute concentration dependence of the local nonideality in the partitioning model is completely damped, any given molecule in the local domain will be completely indifferent to whether its neighboring molecules are solute or water. This corresponds to the situation where $\alpha = 0$ and the ratio $(f_3/f_1)^{local}$ is solute concentration invariant. This special case will be approached when changes in local nonideality become uncorrelated with changes in bulk solution nonideality, as might be observed when there is independent site binding. Indeed, the partitioning model for 1:1 exchange ($S_{1,3} = 1$) is mathematically identical to the competitive 1:1 site binding model in this situation ($\alpha = 0$). Isolated solute molecules bound in recesses or in cavities in the protein would also contribute in a concentration-independent manner to the local activity coefficients. Where solute-protein interactions are weak, α is expected to be positive ($0 < \alpha \leq 1$) because of the concentration dependent interactions between molecules in the local domain, such as would be present in any nonideal liquid. The spectrum of concentration-dependent partitioning behavior for different values of α is summarized in Table 3.

Introduction of local activity coefficients for water and solute into the competitive binding model in a manner analogous to that used here for the solute partitioning model has been proposed—but not implemented—to account for interactions between sites (*13*), perhaps in part because the competitive binding model identifies water and solute molecules bound to the protein surface as integral parts of biopolymer−solute−water complexes (i.e., part of the biopolymer component). Thus, in this model, bound water and solute molecules contribute to the activity coefficients of the ligated states of the biopolymer. By contrast, in the local-bulk

partitioning model, water and solute molecules in the local domain are identified as part of a separate water/solute phase defined by proximity to the protein surface, and it is both appropriate and unambiguous to refer to the chemical potentials (or activity coefficients) of water and solute in this local phase.

Relationship of the Solute Concentration Dependence of K_P to Changes in both Local and Bulk Nonideality. Because K_P is fundamentally the quotient of local and bulk activity coefficients of solute and water (eq 18) and α describes the relationship between the concentration dependence of these activity coefficients, the concentration dependence of K_P is determined by α and by the concentration dependence of the bulk solution activity coefficients. Algebraic manipulation of eqs 18 and 20 yields eq 21 for the derivative of ln K_P with respect to solute concentration

$$\frac{d\ln K_P}{dm_3^{bulk}} \equiv \left.\frac{d\ln(f_3/f_1)^{bulk}}{dm_3^{bulk}}\right|_{m_3^{bulk}=m_3^*} - \alpha K_P(1+\epsilon K_P)\left.\frac{d\ln(f_3/f_1)^{bulk}}{dm_3^{bulk}}\right|_{m_3^{bulk}=K_P m_3^*} \quad (21)$$

where $\epsilon_{KP} \equiv d\ln K_P/d\ln m_3^{bulk}$. If the partition coefficient K_P is observed to be independent of solute concentration (i.e., $d\ln K_P/dm_3^{bulk} = 0$, $\epsilon_{KP} = 0$), then the attenuation factor α relating local and bulk solute activity coefficient derivatives must be inversely related to K_P

$$\alpha = \frac{1}{K_P}\frac{d\ln(f_3/f_1)^{bulk}/dm_3^{bulk}|_{m_3^{bulk}=m_3^*}}{d\ln(f_3/f_1)^{bulk}/dm_3^{bulk}|_{m_3^{bulk}=K_P m_3^*}} \quad (22)$$

For many solutes including GB where the excess chemical potential of the solute (i.e., $\ln(f_3/f_1)$) has an essentially linear dependence on solute molality, eq 22 reduces to $\alpha \cong 1/K_P$. This inverse relationship between K_P and α has important implications for the concentration dependence of K_P for preferentially excluded solutes. For an excluded solute (i.e. $K_P < 1$), a solute concentration independent K_P could only be obtained if the protein enhanced the concentration dependence of solute−solute interactions relative to their bulk solution behavior (i.e., $\alpha > 1$), which is implausible. Thus, we draw the general conclusion that K_P for excluded solutes should be solute concentration dependent. For given values of α and K_P, the greater the solute concentration dependence of bulk solute nonideality, the greater the solute concentration dependence predicted for K_P. For accumulated solutes such as urea, no corresponding prediction regarding the solute concentration dependence or independence of K_P can be made.

A partition coefficient K_P' defined in terms of bulk activities rather than bulk concentrations (cf. eq 4B)

$$K_P' \equiv \frac{(X_3/X_1)^{local}}{(a_3/a_1)^{bulk}} = \frac{X_3^{local}\,a_3^{bulk}}{X_3^{bulk}\,a_3^{local}} \quad (23)$$

is analogous to the exchange constant K_{site} defined in the competitive binding model (eq 12). K_P and K_P' differ by the ratio of bulk activity coefficients

$$K_P = (f_3/f_1)^{bulk}\,K_P' \quad (24)$$

and will therefore be identical only in an ideal solution. Even for the near ideal solute urea (Figure 2), K_P and K_P' differ by as much as 25% near 6 M urea. From eqs 17 and 23,

$$K_P' = \frac{K_{EQ}}{(f_3/f_1)^{local}} = \frac{1}{(f_3/f_1)^{local}} \quad (25)$$

Thus, while K_P is a ratio of bulk to local activity coefficients, K_P' is a function of only the local thermodynamic nonideality. K_P' will be constant *only* in the situation where $(f_3/f_1)^{local}$ is concentration independent (i.e., $\alpha = 0$), corresponding to the relatively unphysical behaviors described above. For weakly perturbing solutes, however, the free energy consequences of protein−solute interactions are similar in magnitude to solute−solute and solute−solvent interactions. In this case, α will differ from zero, and K_P' should in general be solute concentration dependent for any real system.

Application of the Two-Parameter Models to the Dependence of K_{obs} for lacI HTH Unfolding on GB Concentration. The near linear dependence of ΔG°_{obs} (or $\ln K_{obs}$) observed for lacI HTH unfolding on molar GB concentration is fitted remarkably well by the GB partitioning model with two parameters (K_P^o, α) using a regression analysis with a constant value of α. From the fit, $K_P^o = 0.82 \pm 0.01$ (assuming a monolayer of hydration for the local domain) and $\alpha = 0.92 \pm 0.01$. While nonideality in the local domain (unfavorable interactions between GB molecules occupying the local domain) is somewhat attenuated from its bulk solution behavior (the $\alpha = 1$ situation), this attenuation is far from complete (i.e., far from the $\alpha = 0$ situation). Indeed, a model assuming complete attenuation of the concentration dependence of solute and water interactions in the local domain exhibits strong deviations from the data (Figure 4A) even at very low GB concentrations (<0.5 M), as does the competitive binding model applied to the total ASA.

In this analysis, we have used an extended-chain conformation to calculate the maximum ASA of the unfolded state. Use of this maximum ASA is justified by its quantitative utility in correlating heat capacity changes in protein unfolding with the exposure of nonpolar and polar ASA, using heat capacity data and surface areas for exposure of hydrocarbons and amides to water (*37*, *50*, *51*) and in the correlation of denaturant *m*-values and heat capacity changes with surface area (*15*, *22*, *37*). The question of how much residual structure may exist in unfolded proteins under conditions where the unfolded state is stable remains unresolved, however, and the amount of ASA buried in such residual interactions is unknown. To estimate the maximum effect of such residual interactions, we analyzed GB effects on lac I HTH unfolding using a model for the unfolded state ASA based on computationally isolated 17-residue segments of native proteins (*52*), which yields a minimum estimate of the change in ASA upon unfolding of 1564 Å^2. Incorporating this extreme of the possible range of ΔASA into the partitioning model necessarily increases the predicted extent

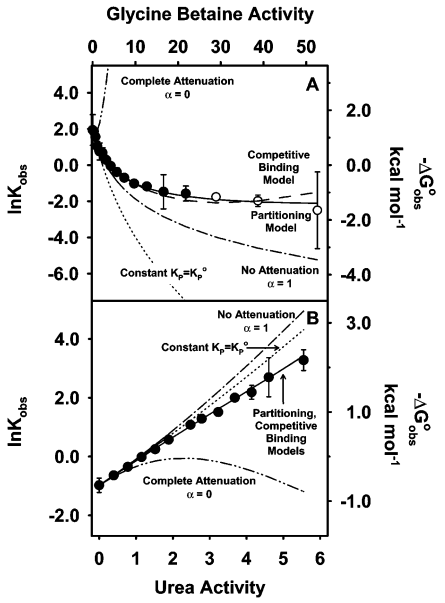

FIGURE 4: The dependence of the equilibrium unfolding of lacI HTH on GB activity (panel A) and urea activity (panel B) is well fit by the two-parameter (K_p^o and α) local-bulk solute partitioning model incorporating local nonideality (—) and the two-parameter (N and K_{site}) independent site 1:1 solute/H_2O binding model (− − −). Curves are also plotted for the α = 1 (− · −), α = 0 (− ·· −), and constant K_P situations (···) fixing K_p^o at 0.82 for GB or 1.12 for urea.

of GB exclusion (yielding $K_p^o = 0.63 \pm 0.01$) and lowers the GB concentration dependence in the local domain (α = 0.78 ± 0.03), but does not otherwise affect any of the above discussion or conclusions.

The competitive binding model (eq 14) with an equal number of parameters (K_{site} and N replace K_P and α) fits the lacI HTH unfolding data satisfactorily (Figure 4A) but not as well as the local-bulk solute partitioning model. In the fit to the competitive binding model, K_{site} is defined analogously to K_P' (eq 23), but refers to only the subset of sites on the total surface exposed upon unfolding. For the surface of lacI HTH exposed upon unfolding, the best fitted values indicate significant preference for binding water instead of GB (K_{site} = 0.16) at a relatively small number of independent sites (N = 44) corresponding to a small fraction of the total surface area (<20%, for any reasonable value of surface area that a single solute molecule may be assumed to occupy). However, the physical significance of N and K_{site} depends on the validity of the thermodynamic treatment of nonideality in the competitive binding model, in which water or solute molecules occupying contiguous sites are considered to be essentially independent.

The value of α obtained from the two-parameter fit to the solute partitioning model predicts that K_P for GB increases with increasing GB concentration (eq 21). For α = 0.92 (obtained using ΔASA = 3465 Å^2), K_P increases from K_p^o = 0.82 at low GB concentrations to ~1.0 at 4 M GB (Figure 5), indicating that in this concentrated GB-biopolymer solution $m_3^{local} \cong m_3^{bulk}$. The increase in the local-bulk GB concentration ratio with increasing GB concentration reduces the amount of additional stabilization of the folded state of lacI HTH at high GB activity, resulting in the plateau (or maximum) in stability observed in Figure 3A. When data are plotted as in a conventional m-value plot (i.e., on the

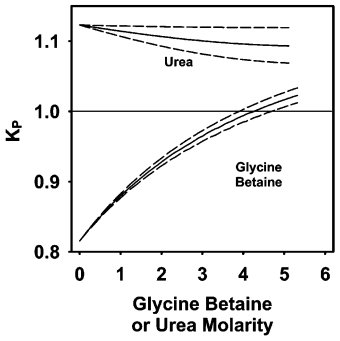

FIGURE 5: The dependence of the partition coefficient K_P (—) on GB and urea concentration from fitted values of α, bracketed by the standard error (− − −) for this quantity. For GB, the concentration at which K_P = 1 is that at which thermodynamic and thermal stability should exhibit maxima (from eq 8 and 26).

molar concentration scale), however, the curvature anticipated from this increase in K_P at high GB concentrations is compensated by the extreme positive nonideality of GB on the molar scale resulting from the imbalance between GB-water interactions (favorable) relative to GB−GB interactions (unfavorable), which leads to an extreme compression of the thermodynamic concentration scale at high molar GB concentrations and produces the observed near-linear dependence of ln K_{obs} on GB molarity. This compensatory effect resulting from the concentration dependence of K_P of GB exclusion from the surface exposed in unfolding also explains the relatively linear dependence of T_m on GB concentration observed for RNase A and lysozyme over the same GB concentration range (0.0−4.0 M) investigated herein (*33*).

Extrapolation of the GB concentration dependence of K_P above 4 M predicts that K_P will intersect unity at ~4.3 M GB (Figure 5) and continue to increase above this GB concentration (i.e., GB is transformed into an accumulated solute as a consequence of GB−GB interactions becoming increasingly more unfavorable in the bulk solution relative to these same interactions in the local domain). Because the transition from exclusion to accumulation involves a sign change in eq 8, this predicted accumulation at very high GB concentrations cannot be compensated simply by compression of the thermodynamic concentration scale of GB nonideality, and thus necessarily predicts a maximum in the thermodynamic stability of the folded protein near 4.3 M and a reduction in the stabilizing effect above this concentration. Parallel treatment of the thermal stability (see below) gives an identical conclusion, in remarkable agreement with the apparent plateau or maximum in plots of T_m vs GB concentration observed by Bolen and co-workers for RNase A and lysozyme near 4 M GB (*33*).

Because GB is known to be excluded from native protein surface (*11*, *49*), the large thermodynamic nonideality of this solute and the premise of attenuation of the solute concentration-dependent bulk nonideality predict a strong increase in K_P with increasing GB concentration for native protein surface as well. We propose that this explains the significant reduction in the efficacy of GB as an osmolyte at high osmolality of growth (and high GB concentration) in vivo, observed by Cayley and Record (*53*). Analysis of the osmotic coefficient of the E. coli cytoplasm as a function of osmolality indicates that K_P values for both GB and other

excluded osmolytes with native protein surface increase with increasing osmolyte concentration in vivo (*53*), in agreement with our in vitro results and theoretical prediction that all excluded solutes should exhibit concentration-dependent partition coefficients at high solute concentration.

Application of the Two-Parameter Models to the Dependence of K_{obs} for lacI HTH Unfolding on Urea Concentration. Application of the concentration dependent K_P model to urea unfolding at 37 °C (Figure 4B) gives $K_P^o = 1.12 \pm 0.02$ and $\alpha = 0.86 \pm 0.12$. This only slightly improves the quality of the fit from the one-parameter (solute concentration invariant K_P) situation because α is within experimental uncertainty of $1/K_P^o = 0.89$, the condition for a concentration independent K_P (eq 22). The greater uncertainty in α for urea (relative to that for GB) is largely due to the fact that the ratio f_3/f_1 for this solute in water decreases from unity by less than 25% in going from dilute solution to 6M (compared to a 440% increase in this ratio as GB concentration is increased to 3 M), and thus the curves representing the $\alpha = 0$ and $\alpha = 1$ situations span a much narrower range for urea than those for GB (Figure 4). The small dependence of f_3/f_1 on urea concentration also results in a much smaller (statistically insignificant) predicted solute concentration dependence of K_P for urea (Figure 5) relative to that for the highly nonideal solute GB, despite the similar fitted values of α for these solutes.

The 1:1 urea−water independent site competitive binding model fits the urea denaturation data as well as the partitioning model, giving $K_{site} = 5.5$ and $N = 10.8$ (corresponding roughly to 5% of the total surface area). Whether these values of K_{site} and N have molecular significance has not been determined; the value of K_{site} obtained herein is about 2-fold larger than that obtained from an analysis of colorimetric studies of unfolded proteins at low pH (*18*), while the ASA-normalized value of N is only one fourth as large as that found previously.

Application of the Solute Partitioning Model to Interpret m-Values and Thermal Denaturation Transitions of Proteins. The dependences of the solute *m*-value and the thermal transition midpoint (T_m) on solute concentration in protein unfolding studies are both directly related to $d \ln K_{obs}/dm_3$ (eq 8) and thus to the preferential interaction of the solute with the affected region of biopolymer surface

$$m\text{-value} = RT\frac{d\ln K_{obs}}{dm_3}\frac{dm_3}{dC_3} \quad (26A)$$

$$\frac{dT_m}{dC_3} = \frac{RT_m^2}{\Delta H^\circ_{obs}(T_m)}\frac{d\ln K_{obs}}{dm_3}\frac{dm_3}{dC_3} \quad (26B)$$

The local-bulk solute partitioning model can be implemented to interpret the dependence of T_m on C_3 by utilizing eqs 8 and 21 for the dependence of ln K_{obs} on solute concentration. While, in general, determination of K_P from the resulting expression requires knowledge of ΔH°_{obs} at T_m as well as the partial molar volumes and two-component activity coefficients of solute and water as functions of temperature and C_3, the limiting value of K_P at low solute concentration (K_P^o) for the interaction of a solute with the surface exposed upon protein unfolding is readily obtained from

$$K_P^o = 1 - \frac{504.5}{\Delta ASA}\frac{\Delta H^\circ_{obs}(T_m)}{RT_m^2}\left.\frac{dT_m}{dC_3}\right|_{C_3\to 0} \quad (27)$$

where the numerical factor (504.5) is the value of $b_1^o/m_1^\bullet$ assuming a monolayer of hydration. In eq 27, values of T_m and $\Delta H^\circ_{obs}(T_m)$ are approximated by those in the absence of solute, and $d\ T_m/d\ C_3$ is evaluated as the limiting slope at low solute concentration.

Factors affecting the curvature (or lack thereof) of T_m as a function of C_3 include $\Delta H^\circ_{obs}(T_m)/T_m^2$ and $\bar{V}_3$ as well as any significant temperature or solute concentration dependence of solute nonideality, of the amount of water in the local domain ($B_1^o = b_1^o\ \Delta ASA$), and of K_P. Information regarding the temperature dependence of K_P^o can be obtained as described previously for the case of urea (*21*). From the preceding analysis, the C_3 dependence of K_P can be predicted

$$K_P = K_P^o\left[\left(\frac{\gamma_3^m}{a_1}\right)^{bulk}\right]^{1-\alpha} \quad (28)$$

The extent of attenuation of the concentration dependence of bulk nonideality determined by the local-bulk partitioning model is similar for both GB and urea (as measured by the parameter α) despite the very different preferential interactions of these two solutes with protein surface, and corresponds roughly to the fraction of surface of these solutes anticipated to be involved in interactions with the protein surface. If this conclusion is general for solute-biopolymer interactions, K_P can be predicted as a function of solute concentration from K_P^o and the molal activity coefficient of the solute (and water activity) in the absence of biopolymer using eq 28 and setting $\alpha = 0.92 \pm 0.01$. The resulting expression should be useful in predicting and interpreting maxima and minima in thermal stability studies or *m*-value plots, such as that described for GB above. If the parameters K_P^o and α from lacI HTH are representative of other proteins, the partitioning model can predict GB effects on the thermodynamic and thermal stability of all proteins with similar compositions of surface exposed in unfolding.

CONCLUSIONS

The urea concentration dependence of ΔG°_{obs} for lacI HTH unfolding is well modeled as either competitive binding or solute partitioning with a single concentration-independent parameter (K_P or K_{site}) when the local domain is defined to comprise the entire surface exposed in unfolding. For both models, however, the analogous one-parameter analysis of the GB concentration dependence of ΔG°_{obs} fails severely even at moderate GB concentration (<1 M). We conclude that this failure arises from the failure of these models to account properly for the pronounced thermodynamic nonideality of GB. To account for this effect, we extend the solute partitioning model by generalizing the interpretation of K_P to incorporate interactions among solute and water molecules in the vicinity of the protein in the form of local activity coefficients for these species. With this extension, the solute partitioning model quantitatively describes the GB

concentration dependence of lacI HTH unfolding as an attenuation of the GB concentration dependence of f_3/f_1 in the local domain relative to that in bulk solution. This effect causes K_P for GB to increase from 0.83 to 1.0 as the bulk GB concentration increases from 0.25 to 4.0 M, in contrast to the behavior of K_P for interaction of urea with this protein surface, which within experimental uncertainty is urea-concentration invariant ($K_P = 1.12 \pm 0.02$) up to 6 M urea.

ACKNOWLEDGMENT

Circular dichroism data were obtained at the UW Biophysics Instrumentation Facility, which is supported by the University of Wisconsin−Madison and grants BIR-9512577 (NSF) and SIO RR13790 (NIH). We thank Dr. Darrell McCaslin for technical assistance with the CD spectrometer, Drs. Robert Kaptein and Christian Spronk for supplying the recombinant lacI DBD cell strain used in these experiments, Dr. Charles Anderson for valuable discussions and comments, and Dr. John Schellman and a reviewer for their comments on the manuscript.

REFERENCES

1. Record, M. T., Jr., Zhang, W., and Anderson, C. F. (1998) Analysis of effects of salts and uncharged solutes on protein and nucleic acid equilibria and processes: a practical guide to recognizing and interpreting polyelectrolyte effects, Hofmeister effects, and osmotic effects of salts. *Adv. Protein Chem. 51*, 281−353.
2. Timasheff, S. N. (1998) Control of protein stability and reactions by weakly interacting cosolvents: The simplicity of the complicated. *Adv. Protein Chem. 51 51*, 355−432.
3. Davis-Searles, P. R., Saunders, A. J., Erie, D. A., Winzor, D. J., and Pielak, G. J. (2001) Interpreting the effects of small uncharged solutes on protein-folding equilibria. *Annu. Rev. Biophys. Biomolec. Struct. 30*, 271−306.
4. Parsegian, V. A., Rand, R. P., and Rau, D. C. (2000) Osmotic stress, crowding, preferential hydration, and binding: A comparison of perspectives. *Proc. Natl. Acad. Sci. U. S. A. 97*, 3987−3992.
5. Timasheff, S. N. (2002) Protein−solvent preferential interactions, protein hydration, and the modulation of biochemical reactions by solvent components. *Proc. Natl. Acad. Sci. U. S. A. 99*, 9721−9726.
6. Timasheff, S. N. (1998) In disperse solution, "osmotic stress" is a restricted case of preferential interactions. *Proc. Natl. Acad. Sci. U. S. A. 95*, 7363−7367.
7. Yancey, P. H., Clark, M. E., Hand, S. C., Bowlus, R. D., and Somero, G. N. (1982) Living with Water-Stress − Evolution of Osmolyte Systems. *Science 217*, 1214−1222.
8. Record, M. T., Courtenay, E. S., Cayley, D. S., and Guttman, H. J. (1998) Responses of E-coli to osmotic stress: Large changes in amounts of cytoplasmic solutes and water. *Trends Biochem. Sci. 23*, 143−148.
9. Record, M. T., Courtenay, E. S., Cayley, S., and Guttman, H. J. (1998) Biophysical compensation mechanisms buffering E-coli protein-nucleic acid interactions against changing environments. *Trends Biochem. Sci. 23*, 190−194.
10. Timasheff, S. N. (1993) The Control of Protein Stability and Association by Weak-Interactions with Water − How Do Solvents Affect These Processes. *Annual Rev. Biophys. Biomolec. Struct. 22*, 67−97.
11. Courtenay, E. S., Capp, M. W., Anderson, C. F., and Record, M. T. (2000) Vapor pressure osmometry studies of osmolyte-protein interactions: Implications for the action of osmoprotectants in vivo and for the interpretation of "osmotic stress" experiments in vitro. *Biochemistry 39*, 4455−4471.
12. Schellman, J. A. (1994) The Thermodynamics of Solvent Exchange. *Biopolymers 34*, 1015−1026.
13. Schellman, J. A. (1990) A simple model for solvation in mixed solvents. Applications to the stabilization and destabilization of macromolecular structures. *Biophys. Chem. 37*, 121−140.
14. Schellman, J. A. (1987) Selective Binding and Solvent Denaturation. *Biopolymers 26*, 549−559.
15. Courtenay, E. S., Capp, M. W., Saecker, R. M., and Record, M. T. (2000) Thermodynamic analysis of interactions between denaturants and protein surface exposed on unfolding: Interpretation of urea and guanidinium chloride m-values and their correlation with changes in accessible surface area (ASA) using preferential interaction coefficients and the local-bulk domain model. *Proteins: Struct., Funct., Genet.* 72−85.
16. Record, M. T., Zhang, W. T., and Anderson, C. F. (1998) Analysis of effects of salts and uncharged solutes on protein and nucleic acid equilibria and processes: A practical guide to recognizing and interpreting polyelectrolyte effects, Hofmeister effects, and osmotic effects of salts. *Adv. Protein Chem. 51*, 281−353.
17. Record, M. T., and Anderson, C. F. (1995) Interpretation of Preferential Interaction Coefficients of Nonelectrolytes and of Electrolyte Ions in Terms of a 2-Domain Model. *Biophys. J. 68*, 786−794.
18. Schellman, J. A., and Gassner, N. C. (1996) The enthalpy of transfer of unfolded proteins into solutions of urea and guanidinium chloride. *Biophys. Chem. 59*, 259−275.
19. Scholtz, J. M., Barrick, D., York, E. J., Stewart, J. M., and Baldwin, R. L. (1995) Urea Unfolding of Peptide Helices as a Model for Interpreting Protein Unfolding. *Proc. Natl Acad. Sci. U. S. A. 92*, 185−189.
20. Schellman, J. A. (2003) Protein stability in mixed solvents: A balance of contact interaction and excluded volume. *Biophys. J. 85*, 108−125.
21. Felitsky, D. J., and Record, M. T. (2003) Thermal and urea-induced unfolding of the marginally stable lac repressor DNA-binding domain: A model system for analysis of solute effects on protein processes. *Biochemistry 42*, 2202−2217.
22. Courtenay, E. S., Capp, M. W., and Record, M. T. (2001) Thermodynamics of interactions of urea and guanidinium salts with protein surface: Relationship between solute effects on protein processes and changes in water-accessible surface area. *Protein Sci. 10*, 2485−2497.
23. Kirkwood, J. G., and Buff, F. P. (1951) Statistical mechanical theory of solutions. I. *J. Chem. Phys. 19*, 774−777.
24. Ben-Naim, A. (1992) *Statistical Thermodynamics for Chemists and Biochemists*, Plenum Press, New York.
25. Chitra, R., and Smith, P. E. (2001) Preferential interactions of cosolvents with hydrophobic solutes. *J. Phys. Chem. B 105*, 11513−11522.
26. Yin, M., Palmer, H. R., Fyfe-Johnson, A. L., Bedford, J. J., Smith, R. A. J., and Yancey, P. H. (2000) Hypotaurine, *N*-methyltaurine, taurine, and glycine betaine as dominant osmolytes of vestimentiferan tubeworms from hydrothermal vents and cold seeps. *Physiol. Biochem. Zool. 73*, 629−637.
27. Yancey, P. H. (2001) Water stress, osmolytes, and proteins. *Am. Zool. 41*, 699−709.
28. Bedford, J. J., Schofield, J., Yancey, P. H., and Leader, J. P. (2002) The effects of hypoosmotic infusion on the composition of renal tissue of the Australian brush-tailed possum Trichosurus vulpecula. *Comp. Biochem. Physiol., Part B*: *Biochem. Mol. Biol. 132*, 645−652.
29. Bedford, J. J., Harper, J. L., Leader, J. P., Yancey, P. H., and Smith, R. A. J. (1998) Betaine is the principal counteracting osmolyte in tissues of the elephant fish, *Callorhincus millii* (*Elasmobranchii*, *Holocephali*). *Comp. Biochem. Physiol., Part B*: *Biochem. Mol. Biol. 119*, 521−526.
30. Edmands, S. D., Hughs, K. S., Lee, S. Y., Meyer, S. D., Saari, E., and Yancey, P. H. (1995) Time-Dependent Aspects of Osmolyte Changes in Rat-Kidney, Urine, Blood, and Lens with Sorbinil and Galactose Feeding. *Kidney Int. 48*, 344−353.
31. Lewis, B. A., Cayley, S., Padmanabhan, S., Kolb, V. M., Brushaber, V., Anderson, C. F., and Record, M. T. (1990) Natural Abundance N-14 and C-13 NMR of Glycine Betaine and Trehalose as Probes of the Cytoplasm of Escherichia-Coli-K12. *J. Magn. Reson. 90*, 612−617.
32. Arakawa, T., and Timasheff, S. N. (1983) Preferential Interactions of Proteins with Solvent Components in Aqueous Amino-Acid Solutions. *Arch. Biochem. Biophys. 224*, 169−177.
33. Santoro, M. M., Liu, Y. F., Khan, S. M. A., Hou, L. X., and Bolen, D. W. (1992) Increased Thermal-Stability of Proteins in the Presence of Naturally-Occurring Osmolytes. *Biochemistry 31*, 5278−5283.
34. Anjum, F., Rishi, V., and Ahmad, F. (2000) Compatibility of osmolytes with Gibbs energy of stabilization of proteins. *Biochim. Biophys. Acta 1476*, 75−84.

35. Yancey, P. H., and Somero, G. N. (1979) Counteraction of urea destabilization of protein structure by methylamine osmoregulatory compounds of elasmobranch fishes. *Biochem. J. 183*, 317−323.
36. Anderson, C. F., Felitsky, D. J., Hong, J., and Record, M. T. (2002) Generalized derivation of an exact relationship linking different coefficients that characterize thermodynamic effects of preferential interactions. *Biophys. Chem. 101*, 497−511.
37. Myers, J. K., Pace, C. N., and Scholtz, J. M. (1995) Denaturant m-values and heat capacity changes − Relation to changes in accessible surface areas of protein unfolding. *Protein Sci. 4*, 2138−2148.
38. Schellman, J. A. (2002) Fifty years of solvent denaturation. *Biophys. Chem. 96*, 91−101.
39. Smith, P. K., and Smith, E. R. B. (1940) Thermodynamic properties of solutions of animo acids and related substances. V. The activities of some hydroxy- and *N*-methylanimo acids and proline in aqueous solution at twenty-five degrees. *Journal of Biological Chemistry 132*, 57−64.
40. Klotz, I. M., and Rosenberg, R. M. (2000) *Chemical Thermodynamics*, 6th ed., John Wiley & Sons, New York.
41. Tsodikov, O. V., Record, M. T., Jr., and Sergeev, Y. V. (2002) Novel computer program for fast exact calculation of accessible and molecular surface areas and average surface curvature. *J. Comput. Chem. 23*, 600−609.
42. Livingstone, J. R., Spolar, R. S., and Record, M. T. (1991) Contribution to the Thermodynamics of Protein Folding from the Reduction in Water-Accessible Nonpolar Surface-Area. *Biochemistry 30*, 4237−4244.
43. Weatherly, G. T., and Pielak, G. J. (2001) *Second virial coefficients as a measure of protein−osmolyte interactions*. *Protein Sci. 10*, 12−16.
44. Edward, J. T. (1970) Molecular volumes and the Stokes−Einstein equation. *J. Chem. Educ. 47*, 261−270.
45. Bevington, P. R., and Robinson, D. K. (1992) *Data Reduction and Error Analysis for the Physical Sciences*, 2nd ed., WCB McGraw-Hill, Boston.
46. Santoro, M. M., and Bolen, D. W. (1992) *A test of the linear extrapolation of unfolding free energy changes over an extended denaturant concentration range*. *Biochemistry 31*, 4901−4907.
47. Johnson, C. M., and Fersht, A. R. (1995) Protein stability as a function of denaturant concentration: ther thermal stability of barnase in the presence of urea. *Biochemistry 34*, 6795−804.
48. Nicholson, E. M., and Scholtz, J. M. (1996) Conformational stability of the *Escherichia coli* HPr protein: Test of the linear extrapolation method and a thermodynamic characterization of cold denaturation. *Biochemistry 35*, 11369−11378.
49. Arakawa, T., and Timasheff, S. N. (1983) Preferential interactions of proteins with solvent components in aqueous amino acid solutions. *Arch. Biochem. Biophys. 224*, 169−177.
50. Spolar, R. S., Livingstone, J. R., and Record, M. T., Jr. (1992) Use of liquid hydrocarbon and amide transfer data to estimate contributions to thermodynamic functions of protein folding from the removal of nonpolar and polar surface from water. *Biochemistry 31*, 3947−3955.
51. Spolar, R. S., and Record, M. T., Jr. (1994) Coupling of local folding to site-specific binding of proteins to DNA. *Science 263*, 777−784.
52. Creamer, T. P., Srinivasan, R., and Rose, G. D. (1997) Modeling unfolded states of proteins and peptides. II. Backbone solvent accessibility. *Biochemistry 36*, 2832−2835.
53. Cayley, S., and Record, M. T., Jr. (2003) Roles of Cytoplasmic Osmolytes, Water, and Crowding in the Response of *Escherichia coli* to Osmotic Stress: Biophysical Basis of Osmoprotection by Glycine Betaine. *Biochemistry 42*, 12596−12609.

BI049862T